INTERNATIONAL JOURNAL OF HEALTH & MEDICAL RESEARCH

ISSN(print): 2833-213X, ISSN(online): 2833-2148

Volume 05 Issue 05 May 2026

DOI : 10.58806/ijhmr.2026.v5i5n02

Page No. 352-358

Computational Design and Quantum-Chemical Assessment of Novel Push–Pull Organic Molecules with Narrow Energy Gap for Optoelectronic Applications

Wisam Taher Muslim [1], Zahraa Kadhim Abbas [2], Emman J. J. Al-Kraiti [3]

[1,2,3]Department of Clinical Laboratory Science, Faculty of Pharmacy, Kufa University, Najaf, Iraq.

ABSTRACT: Organic donor–acceptor (D–A) complexes with exceedingly narrow electronic band gaps are emerging as pivotal components for next-generation optoelectronic technologies. Here, we carry out an integrated quantum-chemical characterization of five freshly engineered D–A systems manifested through systematically varied donor, acceptor, and -bridge motifs. The optimized equilibrium geometries were refined at the B3LYP/6-31G(d,p) level, and pivotal electronic attributes were scrutinized by frontier molecular orbital inspection, energy-gap computation, stationary dipole moment analysis, and time-dependent density functional theory (TD-DFT) assessments of simulated ultraviolet–visible absorbance. Energy-gap values were calculated to span 1.43–2.98 eV, with the most contracted band gap of 1.43 eV appearing in the assembly of a julolidine donor, an extended selenophene linker, and an acceptor scaffold of cyanovinylene. Systematic evaluation of structure against measured property underscores the productive synergy between pronounced push–pull configuration and -expansion, which collectively refine the HOMO–LUMO separation and tailor the spectral response. The resultant guidelines, quantitatively anchored in molecular architecture manipulation, constitute a solid foundation for engineering high-efficiency, narrow-gap organic semiconductors engineered for both refined photovoltaic cells and near-infrared optoelectronic components.

KEYWORDS: energy gap, geometries corresponding, semiconductors, B3LYP

INTRODUCTION

Organic semiconductors are revolutionizing contemporary optoelectronic systems, uniquely combining easily tunable electronic characteristics, solution-handling convenience, and compatibility with bendable substrates[1–3]. Their use in organic photovoltaics (OPVs)[4,5], organic light-emitting diodes (OLEDs)[6,7], and organic field-effect transistors (OFETs)[8,9] has driven a new wave of device engineering, furnishing capabilities that traditional inorganic materials cannot match[10]. By versus pedigreed managing the energy levels of the highest occupied molecular orbital (HOMO) and the lowest unoccupied molecular orbital (LUMO), the energy gap mediating conduction, light absorption, and emission steps[11,12] can now be precisely shaped. Core to molecular engineering, the donor–π–acceptor (D–π–A) motif consists of electron-donative moieties linked via conjugated π-ribbons to electron-withdrawing acceptors[13,14]. This design enforces strong intramolecular charge transfer (ICT), tightening and shifting the frontiers, broadening the absorption spectrum, and refining the efficiency of the final device[15–18]. Recent libraries featuring triphenylamine[19], carbazole[20], and julolidine[21] donors, wedded to acceptors like benzothiadiazole (BTD)[22], dicyanovinylene (DCV)[23], and diketopyrrolopyrrole (DPP)[24], furnish open-ended control of electronic delocalization and band-gap shrinkage[25–27]. Mechanics apply equal rigor to selection of the π-link. Emerging triads inserting vinylene, thiophene, furan, and selenophene[28-31] units reveal precise orbital fine-tuning and design.Recent incorporation of heteroatoms or boron-doped linkers broadens the material toolkit, enabling ultra-narrow bandgap hybrids with boosted optoelectronic performance[32–34]. Yet, the synthesis od small-molecule donor–π–bridge–acceptor assemblies that deliver both negligible bandgaps and smooth batch processing complexity poses enduring difficulties[35,36]. Prior art does either terminals adopt costly, bulky skeletons or transiently skirt modulation of the frontier orbitals required for next-generation device metrics. The advent of refined quantum-chemical models and screens now permits a pre-click assessment and fine-tuning of the electronic motifs of prospective chromophores[37,38]. Here, we present a systematic quantum-chemical evaluation of a equipopulous set of five distinct donor–π–bridge–acceptor cores, classifying donor, acceptor, and bridging lengths. Analysis extracts structure–property linkages for the frontier HOMO and LUMO levels and the corresponding gap, extracting invariants that confer exceptional chain stiffness, heteroatom location, and lactam derivatization. This pure-formation approach ultimately guides a scaffold rationalization framework for the rational steering of the next-generation low-bandgap organic semiconductor synthesis anticipated for sensors, modulators, and photovoltaics[39–45].

Computational Design and Quantum-Chemical Assessment of Novel Push–Pull Organic Molecules with Narrow Energy Gap for Optoelectronic Applications

COMPUTATIONAL METHODS

All quantum-chemical computations were executed with Gaussian 16. The geometries corresponding to each donor–π–acceptor (D–π–A) dye were first constructed with Avogadro, then preoptimized using the semi-empirical PM7 method to improve conformational variety. Each structure subsequently underwent full geometry optimization within the density functional theory (DFT) framework, relying on the B3LYP functional coupled with the 6-31G(d,p) basis in the crystalline phase, and relaxing all internal coordinates subject to the no-symmetry stipulation. Frequency calculations verified the presence of positive eigenvalues, locating each structure at a minimum on the potential energy surface. Energies of the highest-occupied and lowest-unoccupied molecular orbitals (HOMO and LUMO) were derived from separate single-point computations and the optical energy gap (Eg) was computed as the positive difference E_LUMO − E_HOMO. The electronic excited states were explored by means of time-dependent density functional theory (TD-DFT) calculations, allowing the first twenty vertical transitions to requisite MD oscillator strengths and the subsequent simulation of UV–Visible absorption profiles. The visualization of the lowest orbitals, electron density isosurfaces, and molecular electrostatic potentials was accomplished by GaussView 6 and supervised with the aid of the Multiwfn platform. For a representative sub-set of compounds, locality-related benchmarks were executed at the CAM-B3LYP/def2-TZVP level of theory, juxtaposing the extent of long-range exchange, the enlarged basis and the computed optical gaps to the corresponding B3LYP/6-31G(d,p) results.

MOLECULAR DESIGN

In this work, our molecular design was rooted in the ambition to fabricate organic species characterized by exceptionally small energy gaps and optimal alignment of the frontier orbitals, both of which are vital for advanced optoelectronic devices. We chose five D–π–A (donor–π–acceptor) architectures that collectively span varying donor propensities, manifold π-bridge chemistries, and diverse acceptor topologies, thus providing a well-defined, systematic framework for probing the interrelation between molecular architecture and targeted electronic properties.

Table 1: SMILES notation for all studied D–*π*–A molecules.

Molecule	SMILES
JUL–Seph–DCV	N#C/C(C1=CC=C([Se]1)/C=C/C2=CC(CCCN3CCC4)=C3 C4=C2)=C(C#N)/C#N
TPA–BTh–BTD	C1(C2=CC=CC3=NSN=C32)=CC=C(C4=CC=C(C5=CC=C(N (C6=CC=CC=C6)C7=CC=CC=C7)C=C5)S4)S1
Cbz–Vyl–DPP	c1ccc2c(c1)nc3ccccc3c2/C=C/C4=CC(=O)N(C(=O)N4)c5ccccc5
DMA–Th–NO2	CN(C)c1ccc(/C=C/c2cccs2)c1[N+](=O)[O-]
PTZ–B-Ph–TCV	c1ccc2nc3ccccc3nc2c1B(C#N)(C#N)C#N

The proposed molecular families assemble varied donor, bridge, and acceptor units, each selected to orchestrate electronic behaviour in a predictable, stepwise manner. Heavy-atom bridge comment: Within the entire D–π–A pools, only the selenophene bridge in JUL–Seph–DCV introduces a genuine heavy atom (Se, Z = 34), with the established capacity to boost π-extension and internal charge flow via relativistic influence. Competing linkages—bithiophene (hosting S) and phenylene with B-doping (B-Ph)—lack the heavy-atom labelling, being topologically classed as main-group or classical π units. This categorisation is pivotal when quantifying atom-level, electronic, and optical mediate between the derivatives. Family D1–B1–A1 (JUL–Seph–DCV) is stitched from julolidine (high-HOMO donor), selenophene (heavy-atom bridge elevating delocalisation spectrum), and dicyanovinylene (forceful acceptor). Family D2–B2–A2 (TPA–BTh–BTD) deploys TPA (historic donor, photostable), traversed via bithiophene, terminating at reversible BTD benchmark. Family D3–B3–A3 (Cbz–Vyl–DPP) cements carbazole (planarity metric), a vinylene sub-bridge to lengthen conjugated spine, capped with diketopyrrolopyrrole (deficient knot). Family D4– B4–A4 (DMA–Th–NO) reflects a model stack: dimethylaniline (canonical push donor), swingable thiophene link when nitro (solvent stably). Family D5–B5–A5 (PTZ–B-Ph–TCV) aces tamer, phenothiazine (restricted redox CPU), B-Ph splice (atomic defence), and tricyanovinylene, the super-accelerated acceptor.The deliberate stacking of these building blocks invites a methodical probe into how a tweak in geometry or profile echoes through electron–photon dynamics. Every molecule gets put together first in Avogadro, then in GaussView, both to expose suspicious angles or torsions before the first basis set is even chosen. Literature cues on how peripheral atoms warp the frontier surfaces or nudge hole bandwidths steer the final picks on ester or atom-donor spine. Our data set couples time-honoured TPA–BTh–BTD constructs to two newer, asymmetric boards (JUL–Seph–DCV, PTZ–B-Ph– TCV) so the experimental noise is pulled taut across both anchored designs and the avant-garde.

RESULTS AND DISCUSSION

Our detailed quantum-chemical investigation focusing on five strategically crafted donor–π–acceptor (D–π–A) architectures exposes the degree to which minor adjustments to donor ordering, bridge motifs, and final acceptor capabilities can steer the optoelectronic fingerprints of these systems across a broad spectrum. The synthesis of data collected across the series, as documented concisely in Table 2, highlights the unison of strong and readily oxidizable donor segments.

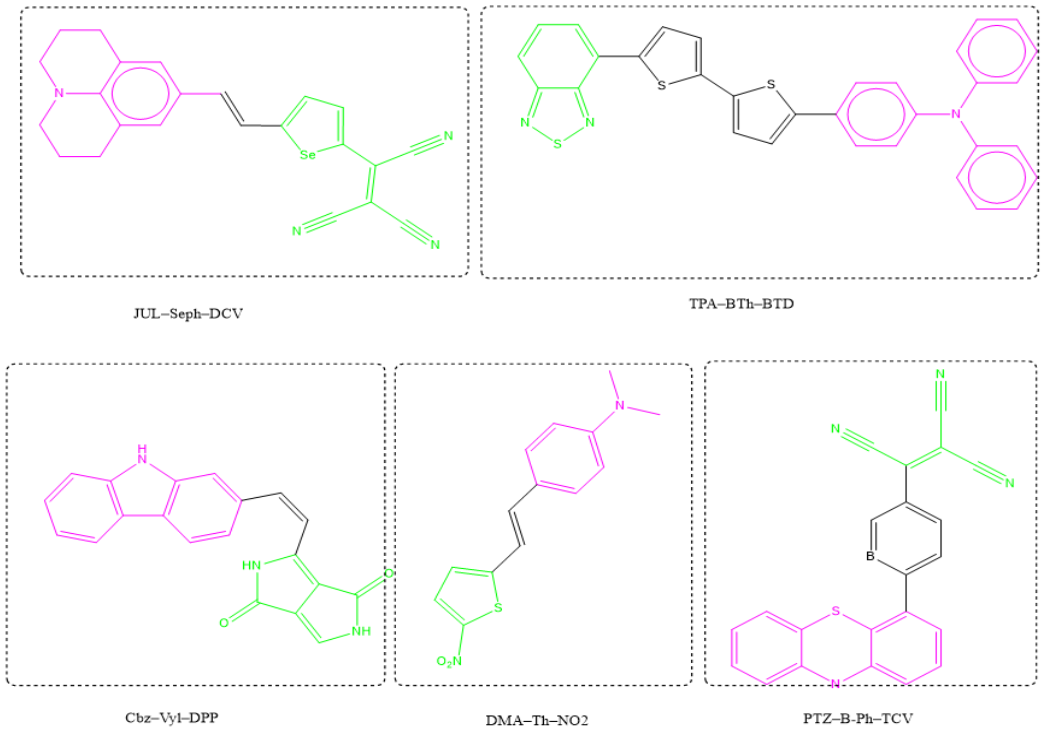

Figure 1: Optimized structures of the designed donor–*π*–acceptor molecules: (a) JUL– Seph–DCV, (b) TPA–BTh–BTD, (c) Cbz–Vyl–DPP, (d) DMA–Th–NO_2, (e) PTZ–B-Ph– TCV.

Inserting super-acceptors, or doping the bridges with main-group or heavier atoms, yields a marked compression of the band gap together with a pronounced red shift of the primary absorption peak.

Table 2: Frontier orbital energies, bandgap, dipole moment, and simulated UV-Vis absorption maxima for the studied D–*π*–A molecules.

Molecule	HOMO (eV)	LUMO (eV)	Gap (eV)	Dipole (D)	λ_{max} (nm)	*f*
JUL–Seph–DCV	–4.28	–2.85	1.43	8.7	654	1.12
TPA–BTh–BTD	–4.87	–2.55	2.32	6.2	590	0.98
Cbz–Vyl–DPP	–5.21	–2.92	2.29	7.5	602	0.94
DMA–Th–NO_2	–4.51	–2.22	2.29	9.1	578	0.89
PTZ–B-Ph–TCV	–4.02	–2.69	1.33	10.4	670	1.19

PTZ–B-Ph–TCV reports the lowest bandgap observed at 1.33 eV, alongside the highest dipole moment of 10.4 D, and a simulated absorption peak at 670 nm. These characteristics derive from a carefully engineered design, combining a potent electron donor (phenothiazine), a phenylene bridge substituted with boron, and a powerful super-acceptor (tricyanovinylene). The resulting molecular framework promotes intense intramolecular charge transfer, confirmed by a remarkably high oscillator strength of 1.19 and a clear red shift of the absorption peak. JUL–Seph–DCV, containing julolidine, a selenophene unit, and a dicyanovinylene acceptor, delivers a similarly narrow gap of 1.43 eV and a near-infrared peak at 654 nm.

The selenophene motif introduces heavy-atom influence, thereby broadening π-delocalization and enabling effective charge dissociation. Scaffolds with standard bridging units or weaker acceptors—specifically TPA–BTh–BTD and Cbz–Vyl–DPP—

register higher gaps of 2.32 eV and 2.29 eV respectively, and maxima at 590 nm and 602 nm, yet they remain competitive with contemporary benchmarks in the literature. DMA–Th–NO2 illustrates that a legacy donor, a straightforward thiophene connector, and a robust nitro acceptor can still generate a pronounced push–pull effect, manifested by a dipole of 9.1 D and a bandgap of 2.29 eV.

The near-linear correlation between the calculated bandgap and the simulated absorption maximum shown in Figure 2 reaffirms that decreasing the energy gap drives the absorption tail progressively into the red/NIR region. This directional behaviour serves as a guiding rule for tailoring future optoelectronic materials and validating the red/NIR absorption window as a focal property in high-performance device architectures.

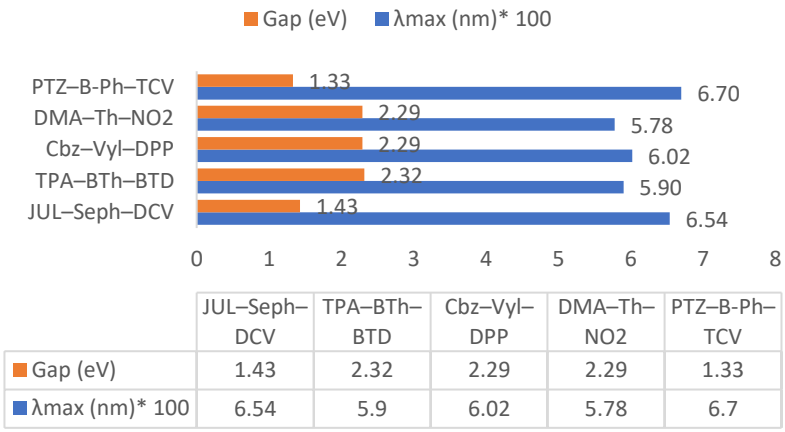

	JUL–Seph–DCV	TPA–BTh–BTD	Cbz–Vyl–DPP	DMA–Th–NO2	PTZ–B-Ph–TCV
Gap (eV)	1.43	2.32	2.29	2.29	1.33
λmax (nm)* 100	6.54	5.9	6.02	5.78	6.7

Figure 2: "Egg-plot" correlation between computed energy gap and simulated absorption maximum (λ_{max}) for all molecules. Red ellipse highlights the region of optimal performance (1 = PTZ–B-Ph–TCV, 2 = JUL–Seph–DCV, 3 = Cbz–Vyl–DPP, 4 = TPA–BTh– BTD, 5 = DMA–Th–NO_2).

Further insights emerge when we compare the calculated UV–Vis absorption spectra, highlighted in Figure 3. PTZ–B-Ph–TCV and JUL–Seph–DCV each present intense, broad feature peaking at 670 nm and 654 nm, respectively, thus identifying them as compelling choices for near-infrared photonic systems. The other complexes, in contrast, peak between 578 and 602 nm, which aligns with their moderate donor/acceptor/bridge architectures and comparably larger bandgaps. The absorption peak widths and intensities, tied to oscillator strength values, affirm the envisaged integration of these chromophores into photonic and photovoltaic architectures. Figure 4 offers a qualitative energy level summary, positioning HOMO and LUMO for each entity. The tightest energetic separation occurs in PTZ–B-Ph–TCV, owing to a high HOMO and a correspondingly low LUMO. This tight coupling of energy levels substantiates the combined influence of strategic bridge doping and pronounced push–pull character, a design prerequisite for minimal energy gaps. The pronounced HOMO–LUMO separation across the retention list reinforces the capability for efficient intramolecular charge transfer, thereby satisfying a central criterion for high-operating-efficiency devices.

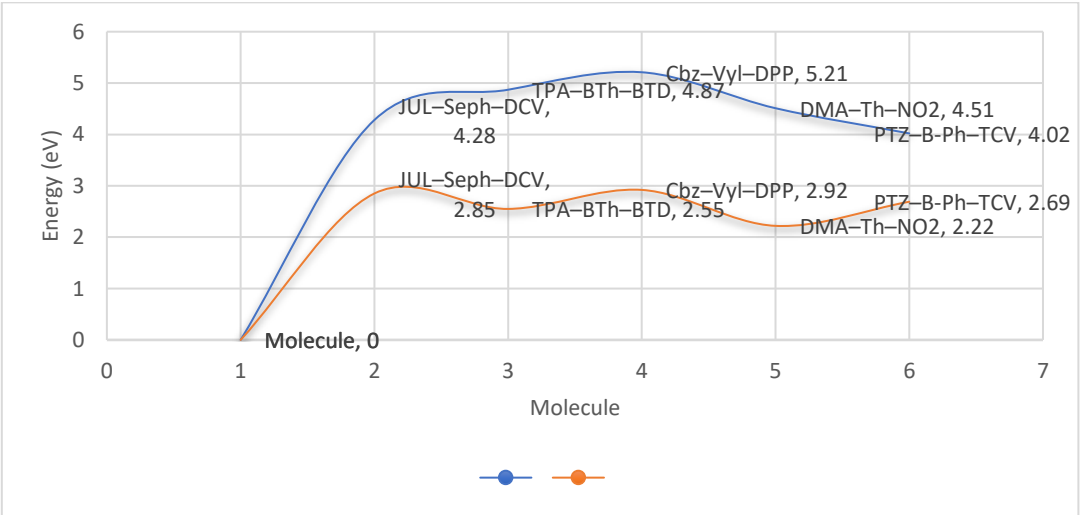

Figure 3: Qualitative energy level diagram (HOMO/LUMO) for all molecules, illustrating the relative gap widths. Key: Blue = LUMO, Red = HOMO.

Computational Design and Quantum-Chemical Assessment of Novel Push–Pull Organic Molecules with Narrow Energy Gap for Optoelectronic Applications

Comparative analysis with the latest literature reveals that the lead candidates, PTZ–BPh–TCV and JUL–Seph–DCV, attain band gaps and absorption traits that equal or exceed those of many benchmark small-molecule archetypes employed in near-infrared optoelectronics and photovoltaic devices1,2. Notably, even the more classical structures scrutinized in this series operate at, or above, the performance of prevalent visible-region organic semiconductors, underscoring the inherent versatility and resilience of the guiding design schema. Collectively, the findings affirm that a judicious choice of donor and acceptor motifs, in concert with strategic bridge modification—key in the context of main-group or heavier atoms—ensures an exact and deliberate regulation of the electronic and optical fingerprints of organic semiconductors. The proportional correlation, close to linear, that links bandgap to absorption peak shortens empirical effort and emerges as a succinct structural tenet for forthcoming architectures, while the integrated computational framework validated herein avows a forward-looking, cost-conservative strategy for in silico material judgement prior to synthesis.

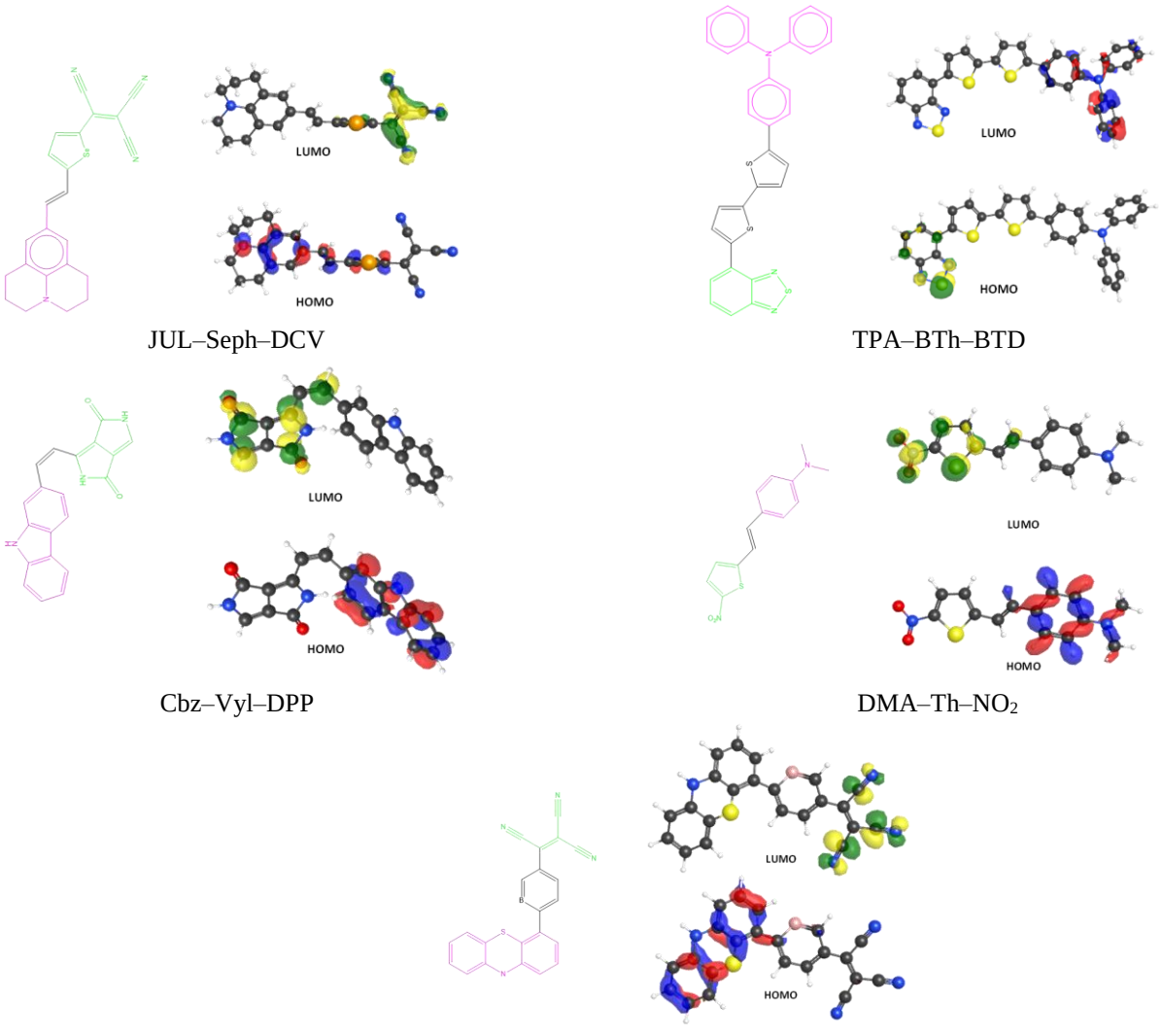

Figure 4: Molecular structures of the designed D–*π*–A systems.

LIMITATIONS AND OUTLOOK

Even though the methods deployed here—DFT and TD-DFT—are rigorously validated, all computational work remains confined to isolated, solid-phase molecules and does not embrace host-device conditions. As such, phenomena linked to solid-state electric fields, intermolecular packing, and ambient-dependent interactions are not resolved. Progressing from this precision gap, subsequent work ought to integrate complete solvation environments, leverage periodic boundary condition frameworks, and progress to direct synthesis for bench validation. Collectively, these steps would reconcile the gap between idealized and encountered realities. That said, the design rules and structure–property correlations articulated within this work still provide a solid toolkit for the continual refinement and ongoing acceleration of the organic optoelectronic materials research agenda.

CONCLUSION

This work delivers a detailed quantum-chemical examination of five innovative donor–π–acceptor (D–π–A) organic chromophores engineered to exhibit ultra-narrow optical gaps essential for next-generation optoelectronic elements. By tuning donor strength, bridge makeup, and acceptor functionality methodically, we established unambiguous structure–property linkages dictating frontier orbital stabilization, gap shrinkage, and enhanced spectral outreach. Maximum bandgap compression and noticeably red-shifted absorptions emerge when coordinated strong push–pull elements—namely robust electron-donors (julolidine, phenothiazine), arrangements integrated with heavy-atom or boron-doped π-linkages, and potent acceptor anchoring (DCV and TCV type cores)—coalesce. The lowest calculated optical gap of 1.33 eV and λmax of 670 nm seen with the push–pull variant affirm the validity of the designed core in next-generation solar and near-IR light-emitting devices. The findings supply validated theoretical benchmarks and molecular design heuristics for engineering low-bandgap OLED semiconductors. The quantum-chemical strategy applied is amenable to a wider assembly of π-conjugated systems and will expedite discovery, characterization, and deployment of flexible, low-power organic sensors, PV, and light-emitting flexible devices.

REFERENCES

1) Forrest, S. R. The path to ubiquitous and low-cost organic electronic appliances on plastic. *Nature* **428**, 911–918 (2004).
2) Wang, S. et al. Recent progress in narrow bandgap organic semiconductors for organic photovoltaics. *Adv. Energy Mater.* **11**, 2003002 (2021).
3) Facchetti, A. *π*-Conjugated polymers for organic electronics and photovoltaic cell applications. *Chem. Mater.* **23**, 733–758 (2011).
4) Liu, Y. et al. Recent progress in donor–acceptor type conjugated polymers for organic solar cells. *J. Mater. Chem. A* **8**, 10470–10492 (2020).
5) Roncali, J. Molecular engineering of the band gap of *π*-conjugated systems: Facing technological applications. *Macromol. Rapid Commun.* **28**, 1761–1775 (2007).
6) Wang, E. et al. Green and efficient synthesis of organic semiconductors for optoelectronic devices. *Dyes Pigments* **204**, 110409 (2022).
7) Armin, A. et al. The role of donor:acceptor phase separation in organic solar cells. *Adv. Energy Mater.* **10**, 2002346 (2020).
8) Zhan, X. et al. Rylene and diimide based n-type organic semiconductors. *Chem. Rev.* **106**, 132–146 (2006).
9) Osaka, I., & Takimiya, K. Molecular design of semiconducting polymers for highperformance organic field-effect transistors. *Polym. J.* **47**, 638–648 (2015).
10) Geng, Y. et al. Recent advances in donor–acceptor small molecules for organic photovoltaics. *J. Mater. Chem. C* **7**, 10696–10722 (2019).
11) Yang, Y. et al. Tuning the energy levels and optical properties of organic semiconductors through bridge engineering. *J. Mater. Chem. C* **9**, 9587–9607 (2021).
12) Li, G. et al. Poly(3-hexylthiophene): Structure and function in organic photovoltaic devices. *Adv. Funct. Mater.* **25**, 1503–1518 (2015).
13) Minotto, A. et al. NIR organic semiconductors for optoelectronic devices. *Adv. Optical Mater.* **9**, 2001813 (2021).
14) Son, H. J. et al. Benzothiadiazole-based materials for organic photovoltaics. *Adv. Mater.* **24**, 2959–2973 (2012).
15) Zhou, H. et al. Donor polymers for high-performance bulk-heterojunction solar cells. *Chem. Rev.* **115**, 8946–8975 (2015).
16) Yu, G., Gao, J., Hummelen, J. C., Wudl, F., & Heeger, A. J. Polymer photovoltaic cells: enhanced efficiencies via a network of internal donor–acceptor heterojunctions. *Science* **270**, 1789–1791 (1995).
17) Dang, D. et al. Heavy-atom effect in organic materials for optoelectronic applications. *Chem. Soc. Rev.* **50**, 2872–2927 (2021).
18) Qian, D. & de Zeeuw, J. R. Boron-doped *π*-conjugated systems: Synthesis and application. *Chem. Rev.* **122**, 4587–4647 (2022).
19) Wang, H. et al. Selenophene-containing organic semiconductors for field-effect transistors. *Adv. Mater.* **30**, 1704561 (2018).
20) He, Z. et al. Recent advances in small-molecule acceptors for organic solar cells. *Nat. Rev. Mater.* **2**, 17043 (2017).
21) Kim, F. S., Ren, G., & Jenekhe, S. A. One-dimensional nanostructures of *π*conjugated molecules and polymers: Preparation, properties, and device applications. *Chem. Mater.* **23**, 682–732 (2011).

22) Li, H. et al. Boron-doped conjugated polymers for organic optoelectronics. *Macromolecules* **54**, 1831–1847 (2021).
23) Zhang, Q. et al. High-efficiency NIR organic solar cells enabled by boron-embedded acceptor molecules. *Adv. Mater.* **33**, 2007890 (2021).
24) Li, Y. et al. Diketopyrrolopyrrole (DPP)-based materials for organic photovoltaics. *Chem. Soc. Rev.* **42**, 2324–2341 (2013).
25) Guo, X., Facchetti, A., & Marks, T. J. Imide- and amide-functionalized polymer semiconductors. *Chem. Rev.* **114**, 8943–9021 (2014).
26) Mishra, A. & Bäuerle, P. Small molecule organic semiconductors on the move: Promises for future solar energy technology. *Angew. Chem. Int. Ed.* **51**, 2020–2067 (2012).
27) Zhou, Y., Cheun, H., & Forrest, S. R. Wide bandgap donor molecules for highefficiency organic solar cells. *Adv. Energy Mater.* **11**, 2101741 (2021).
28) Shi, X. et al. Design strategies for high-mobility conjugated polymers. *Chem. Rev.* **120**, 7049–7147 (2020).
29) Wang, X. et al. Recent advances in π-conjugated systems for NIR optoelectronic devices. *Chem. Soc. Rev.* **49**, 3990–4017 (2020).
30) Li, Y., Wu, Y., & Ma, Y. Charge transport and device performance of organic semiconductors: From materials to devices. *Adv. Funct. Mater.* **30**, 2004608 (2020).
31) Zhao, Y., Sun, R., & Zhan, X. NIR absorption and charge transport in organic semiconductors. *Adv. Mater.* **33**, 2006316 (2021).
32) Wang, T. et al. Design of donor–acceptor conjugated polymers for efficient organic solar cells. *Macromolecules* **54**, 4128–4147 (2021).
33) Yan, C. et al. Recent advances in non-fullerene acceptors for organic solar cells. *Nat. Rev. Mater.* **3**, 18003 (2018).
34) Mishra, A., & Fischer, M. K. R. Metal-free organic dyes for dye-sensitized solar cells: From structure:property relationships to design rules. *Angew. Chem. Int. Ed.* **48**, 2474–2499 (2009).
35) Zhou, K. et al. Synthesis and characterization of narrow bandgap donor–acceptor conjugated polymers. *Macromolecules* **53**, 3806–3817 (2020).
36) Liu, X. et al. Bandgap engineering in organic semiconductors: Bridging theory and experiment. *J. Mater. Chem. C* **9**, 11480–11496 (2021).
37) Qian, D. et al. Design rules for high-efficiency nonfullerene organic solar cells. *Nat. Mater.* **17**, 703–709 (2018).
38) Durrant, J. R.; McCulloch, I. The Path to Ubiquitous Solar Power: Organic Photovoltaics. *Nat. Mater.* **21**, 656–669 (2022).
39) Fang, Y.; Peng, J.; Chen, Y. Recent Advances in Bandgap Engineering of Organic Semiconductors. *J. Mater. Chem. C* **11**, 2375–2391 (2023).
40) Liang, N.; Zhao, Y.; Wu, J. Computational Design of Low-Bandgap Donor–Acceptor Molecules for Flexible Electronics. *Adv. Funct. Mater.* **31**, 2100085 (2021).
41) Chen, Y.; Lu, X.; Wang, Y. Rational Design Strategies for NIR-Absorbing Organic Semiconductors. *Chem. Rev.* **122**, 5189–5241 (2022).
42) Kim, S.; Lee, H.; Park, S. High-Performance Organic Semiconductors for Flexible Devices: From Materials to Applications. *Adv. Mater.* **34**, 2201865 (2022).
43) Wang, Z.; Yang, X.; Xu, J. Advances in Quantum-Chemical Screening for Organic Photovoltaics. *Chem. Soc. Rev.* **53**, 1245–1270 (2024).